Liquid crystal-doped liquid electrolytes for dye-sensitized solar cell applications

Chi-Yen Huang,[1] Chang-Feng You,[1] Cheng-En Cheng,[2,3] Bi-Cheng Lei,[3] Jia-Cih Jhang,[1] Fang-Cheng Yu,[4] Chen-Shiung Chang,[2] and Forest Shih-Sen Chien[3,*]

[1]*Graduate Institute of Photonics, National Changhua University of Education, Changhua 500, Taiwan*
[2]*Department of Photonics and Institute of Electro-Optical Engineering, National Chiao Tung University, Hsinchu 30010, Taiwan*
[3]*Department of Applied Physics, Tunghai University, Taichung 40704, Taiwan*
[4]*AU Optronics Corp.,No.23,Li-Hsin Rd., Hsinchu Science Park, Hsinchu 300, Taiwan*
**fsschien@thu.edu.tw*

Abstract: We investigate the effects of liquid crystals (LCs) on the power conversion efficiency of dye-sensitized solar cells (DSSCs). The photovoltaic and electrochemical impedance spectra indicate that minute amounts of LC dopant decrease the short-current density of DSSCs because the doped LCs reduce the electrochemical reaction rate between DSSC counter electrode and electrolyte. The doped LCs delay the degradation rates of DSSCs because of the interaction between cyano groups of the doped LCs and organic solvent in the liquid electrolyte. Owing to the molecular interaction, the doped LCs increase the viscosity and stability, thereby inhibiting the evaporation rate of the liquid electrolyte.

OCIS codes: (160.3710) Liquid crystals; (350.6050) Solar energy; (230.2090) Electro-optical devices; (160.5335) Photosensitive materials.

References and links

1. B. O'Regan and M. Gratzel, "A low-cost, high-efficiency solar cell based on dye-sensitized colloidal TiO_2 films," Nature **353**(6346), 737–740 (1991).
2. A. Goetzberger, J. Luther, and G. Willeke, "Solar cells: past, present, future," Sol. Energy Mater. Sol. **74**, 1–11 (2002).
3. S. Yun, H. Zhou, L. Wang, H. Zhang, and T. Ma, "Economical hafnium oxygen nitride binary/ternary nanocomposite counter electrode catalysts for high-efficiency dye-sensitized solar cells," J. Mater. Chem. A Mater. Energy Sustain. **1**(4), 1341–1348 (2013).
4. Q. Wang, J. E. Moser, and M. Grätzel, "Electrochemical impedance spectroscopic analysis of dye-sensitized solar cells," J. Phys. Chem. B **109**(31), 14945–14953 (2005).
5. M. Wu, X. Lin, A. Hagfeldt, and T. Ma, "A novel catalyst of WO_2 nanorod for the counter electrode of dye-sensitized solar cells," Chem. Commun. (Camb.) **47**(15), 4535–4537 (2011).
6. K. M. Lee, W. H. Chiu, M. D. Lu, and W. F. Hsieh, "Improvement on the long-term stability of flexible plastic dye-sensitized solar cells," J. Power Sources **196**(20), 8897–8903 (2011).
7. T. Asano, T. Kubo, and Y. Nishikitani, "Electrochemical properties of dye-sensitized solar cells fabricated with PVdF-type polymeric solid electrolytes," J. Photochem. Photobiol. Chem. **164**(1-3), 111–115 (2004).
8. M. Biancardo, K. West, and F. C. Krebs, "Optimizations of large area quasi-solid-state dye-sensitized solar cells," Sol. Energy Mater. Sol. **90**(16), 2575–2588 (2006).
9. A. R. S. Priya, A. Subramania, Y. S. Jung, and K. J. Kim, "High-performance quasi-solid-state dye-sensitized solar cell based on an electrospun PVdF-HFP membrane electrolyte," Langmuir **24**(17), 9816–9819 (2008).
10. S. Agarwala, L. N. S. A. Thummalakunta, C. A. Cook, C. K. N. Peh, A. S. W. Wong, L. Ke, and G. W. Ho, "Co-existence of LiI and KI in filler-free, quasi-solid-state electrolyte for efficient and stable dye-sensitized solar cell," J. Power Sources **196**(3), 1651–1656 (2011).
11. B. O'Regan and D. T. Schwartz, "Large enhancement in photocurrent efficiency caused by uv illumination of the dye-sensitized heterojunction TiO_2/RuLL'NCS/CuSCN: initiation and potential mechanisms," Chem. Mater. **10**(6), 1501–1509 (1998).
12. G. R. A. Kumara, S. Kaneko, M. Okuya, and K. Tennakone, "Fabrication of dye-sensitized solar cells using triethylamine hydrothiocyanate as a CuI crystal growth inhibitor," Langmuir **18**(26), 10493–10495 (2002).
13. U. Bach, D. Lupo, P. Comte, J. E. Moser, F. Weissortel, J. Salbeck, H. Spreitzer, and M. Grätzel, "Solid-state dye-sensitized mesoporous TiO_2 solar cells with high photon-to-electron conversion efficiencies," Nature **395**(6702), 583–585 (1998).

#255320 Received 14 Dec 2015; revised 28 Feb 2016; accepted 2 Mar 2016; published 4 Mar 2016

14. H. J. Snaith, A. J. Moule, C. Klein, K. Meerholz, R. H. Friend, and M. Grätzel, "Efficiency enhancements in solid-state hybrid solar cells via reduced charge recombination and increased light capture," Nano Lett. **7**(11), 3372–3376 (2007).
15. Y. Yang, H. Hu, C. H. Zhou, S. Xu, B. Sebo, and X. Z. Zhao, "Novel agarose polymer electrolyte for quasi-solid state dye-sensitized solar cell," J. Power Sources **196**(4), 2410–2415 (2011).
16. J. Yoon, D. K. Kang, J. Won, J. Y. Park, and Y. S. Kang, "Dye-sensitized solar cells using ion-gel electrolytes for long-term stability," J. Power Sources **201**, 395–401 (2012).
17. J. Xia, F. Li, C. Huang, J. Zhai, and L. Jiang, "Improved stability quasi-solid-state dye-sensitized solar cell based on polyether framework gel electrolytes," Sol. Energy Mater. Sol. **90**(7-8), 944–952 (2006).
18. P. Wang, S. M. Zakeeruddin, J. E. Moser, and M. Grätzel, "A new ionic liquid electrolyte enhances the conversion efficiency of dye-sensitized solar cells," J. Phys. Chem. B **107**(48), 13280–13285 (2003).
19. K. Yuan, F. Li, L. Chen, Y. Li, and Y. Chen, "Liquid crystal helps ZnO nanoparticles self-assemble for performance improvement of hybrid solar cells," J. Phys. Chem. C **116**(10), 6332–6339 (2012).
20. X. Chen, L. Chen, and Y. Chen, "Self-assembly of discotic liquid crystal decorated ZnO nanoparticles for efficient hybrid solar cells," RSC Advances **4**(7), 3627–3632 (2014).
21. T. Yasuda, H. Ooi, J. Morita, Y. Akama, K. Minoura, M. Funahashi, T. Shimomura, and T. Kato, "Π-conjugated oligothiophene-based polycatenar liquid crystals: self-organization and photoconductive, luminescent, and redox properties," Adv. Funct. Mater. **19**(3), 411–419 (2009).
22. H. K. Kim, M. J. Lee, S. H. Jin, and G. D. Lee, "Optimization of Liquid crystal concentration in the dye-sensitized solar cell for high efficiency," Mol. Cryst. Liq. Cryst. (Phila. Pa.) **510**(1), 323–328 (2009).
23. G. Vijayakumar, M. J. Lee, M. Song, S. H. Jin, J. W. Lee, C. W. Lee, Y. S. Gal, H. J. Shim, Y. Kang, G. W. Lee, K. Kim, N. G. Park, and S. Kim, "New liquid crystal-embedded PVdf-Co-HFP-based polymer electrolytes for dye-sensitized solar cell applications," Macromol. Res. **17**(12), 963–968 (2009).
24. C. E. Cheng, C. Y. Lin, C. H. Shan, S. Y. Tsai, K. W. Lin, C. S. Chang, and F. S. S. Chien, "Platinum-graphene counter electrodes for dye-sensitized solar cells," J. Appl. Phys. **114**(1), 014503 (2013).
25. J. Ptasinski, I. C. Khoo, and Y. Fainman, "Passive temperature stabilization of silicon photonic devices using liquid crystals," Materials (Basel) **7**(3), 2229–2241 (2014).
26. S. Y. Huang, G. Schlichthörl, A. J. Nozik, M. Grätzel, and A. J. Frank, "Charge recombination in dye-sensitized nanocrystalline TiO_2 solar cells," J. Phys. Chem. B **101**(14), 2576–2582 (1997).
27. J. Wu, Z. Lan, J. Lin, M. Huang, and P. Li, "Effect of solvents in liquid electrolyte on the photovoltaic performance of dye-sensitized solar cells," J. Power Sources **173**(1), 585–591 (2007).
28. R. Bajpai, S. Roy, N. kulshrestha, J. Rafiee, N. Koratkar, and D. S. Misra, "Graphene supported nickel nanoparticle as a viable replacement for platinum in dye sensitized solar cells," Nanoscale **4**(3), 926–930 (2012).
29. Q. W. Jiang, G. R. Li, and X. P. Gao, "Highly ordered TiN nanotube arrays as counter electrodes for dye-sensitized solar cells," Chem. Commun. (Camb.) **44**(44), 6720–6722 (2009).
30. G. R. Li, F. Wang, Q. W. Jiang, X. P. Gao, and P. W. Shen, "Carbon nanotubes with titanium nitride as a low-cost counter-electrode material for dye-sensitized solar cells," Angew. Chem. Int. Ed. Engl. **49**(21), 3653–3656 (2010).
31. Y. J. Chang and T. J. Chow, "Highly efficient triarylene conjugated dyes for sensitized solar cells," J. Mater. Chem. **21**(26), 9523–9531 (2011).
32. N. Cho, H. Choi, D. Kim, K. Song, M. S. Kang, S. O. Kang, and J. Ko, "Novel organic sensitizers containing a bulky spirobifluorene unit for solar cell," Tetrahedron **65**(31), 6236–6243 (2009).
33. L. Han, N. Koide, Y. Chiba, and T. Mitate, "Modeling of an equivalent circuit for dye-sensitized solar cells," Appl. Phys. Lett. **84**(13), 2433–2435 (2004).
34. E. Barsoukov and J. R. Macdonald, *Impedance Spectroscopy: Theory, Experiment, and Applications* (Wiley, New Jersey, 2005).
35. S. C. Kim, M. Song, T. I. Ryu, M. J. Lee, S. H. Jin, Y. S. Gal, H. K. Kim, G. D. Lee, and Y. S. Kang, "Liquid crystals embedded in polymeric electrolytes for quasi-solid state dye-sensitized solar cell applications," Macromol. Chem. Phys. **210**(21), 1844–1850 (2009).
36. D. Xu, X. Chen, L. Wang, L. Qiu, H. Zhang, and F. Yan, "Performance enhancement for high performance dye-sensitized solar cells via using pyridinyl-functionalized ionic liquid type additive," Electrochim. Acta **106**, 181–186 (2013).
37. H. Yang, M. Huang, J. Wu, Z. Lan, S. Hao, and J. Lin, "The polymer gel electrolyte based on poly(methyl methacrylate) and its application in quasi-solid-state dye-sensitized solar cells," Mater. Chem. Phys. **110**(1), 38–42 (2008).
38. A. Mathew, G. M. Rao, and N. Munichandraiah, "Towards fabrication of stable dye sensitized solar cells based on acetonitrile as solvent for the redox couple," Adv. Mater. Lett. **5**, 180 (2014).

1. Introduction

Photo-electrochemical dye sensitized solar cells (DSSCs) have attracted considerable attention since the demonstration of O'Regan and Grätzel in 1991. Compared with conventional silicon-based solar cells, DSSCs have the advantages of low cost, low energy consumption, color choice, and high transparency [1–3]. A typical DSSC comprises a dye-sensitized metal oxide semiconductor film as photoactive anode, a good ion-transporting electrolyte, and an efficient counter electrode. Upon photoexcitation, the photo-electrons are

#255320 Received 14 Dec 2015; revised 28 Feb 2016; accepted 2 Mar 2016; published 4 Mar 2016

injected from excited dyes into the conducting band of the metal oxide. The oxidized dyes can be reduced by a redox mediator in the electrolyte located between two electrodes. Moreover, the oxidized electrolyte can be reduced by the electrons injected from the counter electrode [4]. The most commonly used electrolyte in high-efficiency DSSCs usually consists of a triiodide/iodide (I_3^-/I^-) redox couple dissolved in a volatile organic solvent, which has the potential for advanced commercialization [5, 6]. However, the liquid electrolytes used in DSSCs present several technological problems, such as dye desorption, solvent evaporation, dye degradation, Pt desorption of the counter electrode, and leakages of the volatile solvent and the redox couple [7–10]. Consequently, long-term stability is among the main drawbacks of the liquid electrolyte-based DSSCs and needs to be solved. Considerable efforts have been made to replace the liquid electrolyte with a solid-state or a quasi-solid-state electrolyte, such as *p*-type semiconductors [11, 12], organic hole transport medium [13–15], polymer electrolytes [15–17], and ionic liquids [18]. However, the overall conversion efficiencies of these alternatives are still lower than those of DSSCs with liquid electrolytes.

Mesophases of liquid crystals (LCs) exist between crystalline solids and isotropic liquids and have been studied extensively in display applications. Several papers discuss the effects of LCs on the efficiencies of hybrid solar cells and recently [19–21], applications of LCs in DSSCs have been demonstrated. Kim et al. doped LCs into polymer electrolytes [22], where power conversion efficiency (PCE) and fill factor (FF) measurements indicated that the addition of LCs improves the efficiency of DSSCs. Vijayakumar et al. found that the addition of LCs to the conventional polymer electrolyte remarkably enhanced DSSC efficiency by increasing the number of pathways for electron injection and by increasing the dye regeneration rate [23]. To our knowledge, the effects of LC materials on liquid electrolyte-based DSSCs have never been reported. Therefore, we investigate the effects of LC addition on the efficiency of the liquid electrolyte-based DSSCs. A minute amount of LC dopant effectively decreases the degradation rate of liquid electrolyte-based DSSCs. The experimental procedures, obtained results, and possible mechanisms are presented in this study.

2. Experimental details

For the fabrication of DSSCs [24], the photo-anodes were prepared according to the following steps. (1) A P25-TiO_2 dye-absorbed layer was spin-coated on the fluorine-doped tin oxide (FTO) glass. (2) The P25-TiO_2 film was coated with a TiO_2 (R-706, DuPont; ~360 nm in diameter) light scattering layer. (3) The TiO_2 films were sintered at 400 °C in air for 30 min to create porous structure. (4) The thermally treated TiO_2 films were immersed in a 0.2 mM solution of ruthenium dye N719 for 16 h. The Pt-coated FTO glass was employed as counter electrode in this experiment. Finally, as shown in Fig. 1(a), the photo-anode and counter electrode were assembled with 30 μm-thick-spacers (Surlyn, DuPont) in a sandwich type filled with electrolyte. The electrolyte was prepared from 0.5 M LiI and 0.05 M I_2 in 3-methoxypropionitrile (3-MPN; Fig. 1(b), Sigma-Aldrich). 3-MPN has a dielectric constant of ~36 and a viscosity of ~2.5 cps at room temperature [7]. The LC E7 (Fig. 1(c), Merck) was used to dope the liquid electrolyte. E7 comprises four kinds of LC molecules (5CB, 7CB, 80CB, and 5CT) with similar chemical structures. These LC molecules consist of an aromatic-ring-based mesogenic core, a cyano group as terminal group, and a flexible alkyl or alkoxy chain as the spacer. E7 has an extraordinary dielectric constant of ~19.3, an ordinary dielectric constant of ~5.2, and thus an average dielectric constant ~9.9 at room temperature. The viscosity constant of E7 is ~40 cps at room temperature [25]. The same cyano terminal group enhances the intermolecular interaction between LCs and 3-MPN, and the aromatic rings of E7 with cyano groups attached improve the thermal stability of the LC-doped liquid electrolyte. E7 was mixed in the as-prepared electrolyte in ratios of 5, 10, and 15 wt%. The LC-doped electrolytes were filled into transparent cells and placed under the polarized microscope, in which the polarizer and analyzer were crossed. The thickness of the cell was ~25 μm. The observed images were darken when the cells were rotated, which indicated that the LC-doped electrolytes were in the isotropic state, and the mesophases did not exist in the

#255320 Received 14 Dec 2015; revised 28 Feb 2016; accepted 2 Mar 2016; published 4 Mar 2016

LC-doped electrolytes in this experiment. To measure the Tafel curves of the LC-doped electrolytes, two counter electrodes were assembled with 30 μm-thick spacers and filled with the LC-doped electrolytes. In this study, the sample filled with pristine electrolyte was defined as the standard sample.

The Tafel polarization curves and the current density–voltage (*J–V*) curves of the DSSCs were recorded by a current–voltage source meter (Jiehan 5000 electrochemical workstation). The Tafel polarization measurements were employed to confirm the electrocatalytic activity of the electrolytes using symmetrical cells. The *J–V* characteristics of the DSSCs were obtained under the illumination of a Xenon lamp with an air mass (AM) 1.5 G filter. The electrochemical impedance spectra (EIS) of the DSSCs were obtained in the frequency range of 1 Hz to 100 kHz using an LCR meter (HIOKI 3522-50). The EIS spectra of DSSC were used to analyze the carrier dynamics in DSSCs. To accelerate electrolyte degradation, the DSSC samples for the long-term stability measurements were left unsealed and stored in a fume hood in the dark. Thermal property of the LC-doped electrolyte was evaluated using a thermogravimetric analyzer (TGA, TI Instrument). The TGA traces for thermal stability of the LC-doped liquid electrolytes were measured at a heating rate of 10 °C/min under air flow.

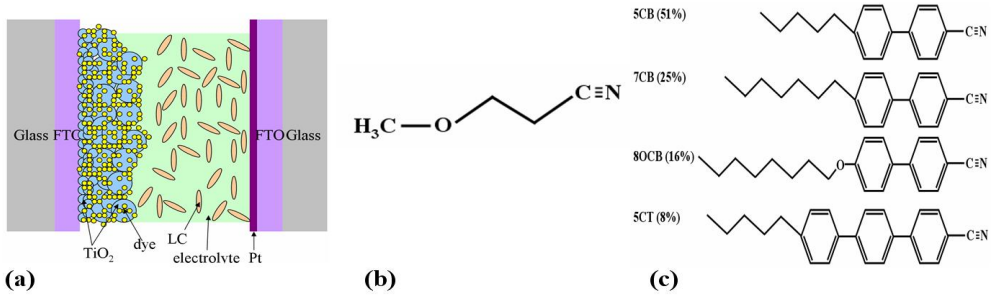

Fig. 1. (a) Schematic of DSSCs containing LC (not to scale), (b) molecular structures of 3-MPN, (c) molecular structures and composition of E7.

3. Results and discussions

Tafel polarization curves were employed to confirm the electrochemical reaction rates of the LC-doped electrolytes. The curve at the low potential (V < 120 mV) is attributed to the polarization zone, whereas the curve at the middle potential (with a sharp slope) is attributed to the Tafel zone. The curve at the high potential (horizontal part) is attributed to the diffusion zone. In the last two zones, we obtain information on exchange current density (J_0) and limiting diffusion current density (J_{lim}) [5]. The Tafel curves of the LC-doped electrolytes are shown in Fig. 2(a). J_0 in the Tafel zone can be obtained by extending the slope of the Tafel polarization curve (i.e., dashed line in Fig. 2(a)) to zero voltage and measuring the intercept on the J axis (Y-axis) [3]. J_0 decreases as LC concentration increases, thereby suggesting that the doped LCs reduce the electrochemical reaction rate of I_3^- reduction. J_{lim} is the saturation current density at high voltage [3], which also decreases as LC concentrations increases, this indicates that the diffusion velocity of a redox couple decreases with increasing LC concentration. The measured *J–V* curves of the LC-doped DSSCs are shown in Fig. 2(b). The calculated photovoltaic parameters of the DSSCs are summarized in Table 1. The short-circuit current density (J_{SC}) decreases with increasing LC concentration, whereas the open-circuit voltage (V_{OC}) is nearly independent of the LC concentration. The photocurrent density (J_{ph}) is given by [26]:

$$J_{ph} = J_{inj} - J_r, \tag{1}$$

where J_{inj} is the electron injection current density resulting from dye sensitization, and J_r is the surface recombination current density. V_{OC} is defined as the voltage at which photocurrent density J_{ph} disappears. The V_{OC} of the DSSCs can be approximated as follows [26, 27]:

#255320 Received 14 Dec 2015; revised 28 Feb 2016; accepted 2 Mar 2016; published 4 Mar 2016

$$V_{OC} = \left[\frac{kT}{q}\right] \ln\left\{\frac{AI_0}{n_0 k_{et} C_{0X}}\right\}, \quad (2)$$

where k is Boltzmann constant, T absolute temperature, q electronic charge, I_0 is incident photon □ux, A is the ratio of absorbed photon to I_0, n_0 is the concentration of electrons in the TiO_2 present in the dark state, and k_{et} is the rate constant for triiodide reduction on TiO_2; and C_{0X} is the concentration of the oxidized half of the redox couple, that is, the I_3^- concentration in electrolyte. n_0, k_{et}, and C_{0X} are parameters that determine the recombination current of the DSSCs. Equation (2) is obtained under some important assumptions [26]. First, the photo-voltage in DSSCs is assumed only to be controlled by the conduction-band electrons, although the recombination current may have come from the localized electrons in surface states and free electrons in the conduction band. Second, the potential drop between the TiO_2 surface and redox electrolyte in the dark state can be neglected because of the nano-porous structures of TiO_2. The addition of LCs reduces I_3^- concentration (C_{0X} in the electrolyte). However, Table 1 shows that V_{OC} is nearly independent of the doped LC concentration, indicating that the ratio of AI_0/n_0k_{et} decreases with increasing LC concentration. The effects of LC dopant on A, I_0, n_0 and k_{et} still require detailed investigations. V_{OC} is independent of the LC concentration, so the decrease in the PCE of DSSCs is mainly attributed to the decrease in current density with the reduction of the electrochemical reaction rate by the doped LCs.

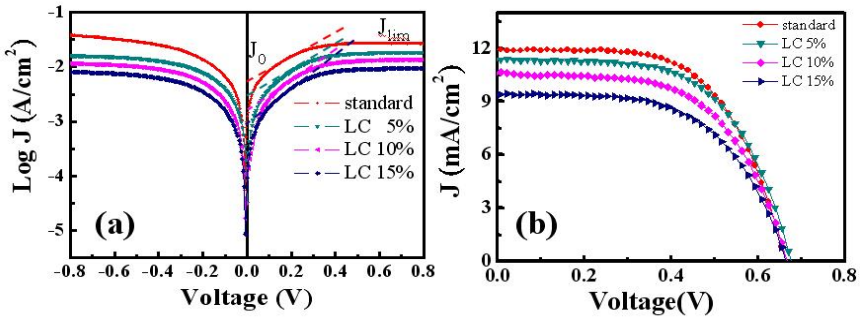

Fig. 2. (a) Tafel polarization curves of the symmetrical cells with various LC concentrations, (b) photovoltaic characteristic curves of the LC-doped DSSCs at various LC concentrations.

Table 1 Photovoltaic parameters of the LC-doped DSSCs at various LC concentrations.

	PCE (%)	Jsc (mA/cm2)	Voc (mV)	FF
Standard	**4.77**	**11.9**	**656**	**0.61**
LC-5%	**4.61**	**11.3**	**671**	**0.61**
LC-10%	**4.14**	**10.7**	**656**	**0.59**
LC-15%	**3.63**	**9.4**	**656**	**0.59**

PCE: power conversion efficiency, JSC: short-circuit current density, VOC: open-circuit voltage, FF: filling factor

The EIS spectra of DSSCs under illumination were obtained to identify their electrochemical behavior. The Nyquist plots of the LC-doped DSSCs are shown in Fig. 3. The impedance spectra were fitted with the equivalent circuit (Inset of Fig. 3) in the frequency range of 1 Hz to 100 kHz using commercially available software Zview. The fitted results are summarized in Table 2. The error between the fitted and measured results in Table 2 is less than 3%. In the equivalent circuit, the series resistance (R_s) describes the bulk resistance [28], including the resistances of the electrodes, electrolyte, and contacts. The charge-transfer resistance (R_{ct}) describes the electrochemical reactions of I_3^-/I^- at the counter electrode [29, 30]. The recombination resistance (R_{rec}) is related to the electron transport process at the TiO_2/electrolyte and TiO_2/dye interfaces [31, 32]. In Fig. 3, R_{ct} is the radius of the semicircle on the left, which indicates the high-frequency responses (>100 Hz) of the DSSCs; and R_{rec} is

#255320 Received 14 Dec 2015; revised 28 Feb 2016; accepted 2 Mar 2016; published 4 Mar 2016

the radius of the semicircle on the right, which indicates the low frequency responses (<100 Hz). The constant phase elements CPE1 and CPE2 represent the non-ideal frequency-dependent capacitances attributed to the non-uniform distribution of current by material heterogeneity [7]. The impedance of the CPE is defined by following equation [33]:

$$Z_{CPE} = \frac{1}{T(i\omega)^{P}}, \tag{3}$$

where T is frequency-independent magnitude and P is phase parameter obtained by curve fitting. The frequencies f_{ct} and f_{rec} at the apexes of the semicircles represent the reduction rate at the counter electrode/electrolyte interface and the recombination rate at the TiO_2/dye/electrolyte interface, respectively. f_{ct} and f_{rec} coincide with the characteristic frequencies of the corresponding parallel R-CPE circuit, and are expressed as follows [34]:

$$f = \frac{1}{2\pi}(R \times T)^{-1/P}. \tag{4}$$

The calculated f_{ct} and f_{rec} are listed in Table 2, which shows that the LC-doped electrolyte cells have lower f_{ct} than standard electrolyte cells. The viscosity of E7 (40 cps) is larger than that of 3-MPN solvent (~2.5 cps), indicating that the addition of E7 increases the viscosity of liquid electrolyte. From the Tafel curves (Fig. 2(a)), the diffusion velocity of the redox couple decreases with increasing LC concentration. The decrease in diffusion velocity reduces the supply of I_3^- to the Pt counter electrode, which thereby depletes the I_3^- concentration at the electrode and reduces the electrochemical reaction rate and PCEs of the DSSCs. Furthermore, the doped LCs reduces the recombination rate of electrons in the TiO_2/dye/electrolyte interface, suggesting that LC material with high resistance suppresses the recombination rate of electrons in the TiO_2/dye/electrolyte interface. As shown in Table 2, the doped LCs increases R_{ct} and consequently decreases J_{SC} and PCE of the DSSCs. However, these results are inconsistent with those in the literature [22, 23], which claim that the addition of LCs generally increases the PCE of the polymer electrolyte-based DSSCs because the doped LCs increase the additional conductive pathways of the polymer electrolyte [23, 35]. The main reason is that the massive LC dopant change the order parameter of the polymer electrolyte. Nonetheless, a minute amount of LC dopant cannot change the order parameter of the liquid electrolyte in our experiment. The nematic phase of LC may affects the PCE of the liquid electrolyte-based DSSCs, but more studies are required.

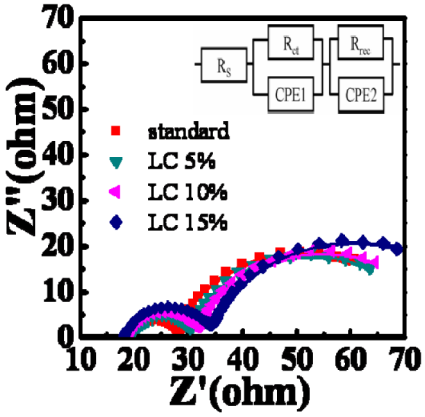

Fig. 3. Nyquist plots of the LC-doped DSSCs at various LC concentrations. The inset presents equivalent circuit of the DSSCs.

#255320 Received 14 Dec 2015; revised 28 Feb 2016; accepted 2 Mar 2016; published 4 Mar 2016

Tab. 2 Impedances of the equivalent circuit components and the characteristic frequencies of the LC-doped DSSCs.

	Rs (Ω)	Rct (Ω)	Rrec (Ω)	CPE1-T (μF)	CPE1-P	fct (Hz)	CPE2-T (μF)	CPE2-P	frec (Hz)
Standard	19	9	45	40.5	0.88	1278	4810	0.87	0.93
LC-5%	19	11	45	37.5	0.89	1065	5020	0.85	0.93
LC-10%	19	13	47	44.4	0.87	877	5650	0.83	0.78
LC-15%	18	15	54	48.2	0.87	627	6010	0.82	0.62

The long-term stability of the LC-doped DSSCs was evaluated by *J–V* measurements. The PCEs and normalized PCEs of the DSSCs are shown as function of time in Figs. 4(a) and 4(b), respectively. The PCEs of the DSSCs decay with time because of the leakage or vaporization of the electrolyte, but the addition of LCs delay the decay rate of the DSSCs (Fig. 4(a)). At 432 hr, the PCE of the DSSC fabricated with standard electrolyte is reduced to ~0%. By contrast, the PCE in the 5 wt% LC-doped cell is still 2%, which is ~40% of the efficiency of the 5 wt% LC-doped sample at 0 hr. Notably, when the doped LC concentration exceeds 5 wt%, the effect of LCs on the long-term stability of DSSCs worsens. At 432 hr, the PCE of the 10 wt% LC doped-DSSCs is 0.7%, which is still higher than that of standard electrolyte DSSCs. The TGA curves of the LC-doped electrolytes are shown in Fig. 4(c). The continuous weight loss of the electrolyte occurs when the temperature increases because the 3-MPN solvent in the electrolyte evaporates [36]. Notably, the addition of LCs retards the weight loss of the electrolytes, and the electrolyte with 5 wt% LC concentration shows the slowest weight loss rate.

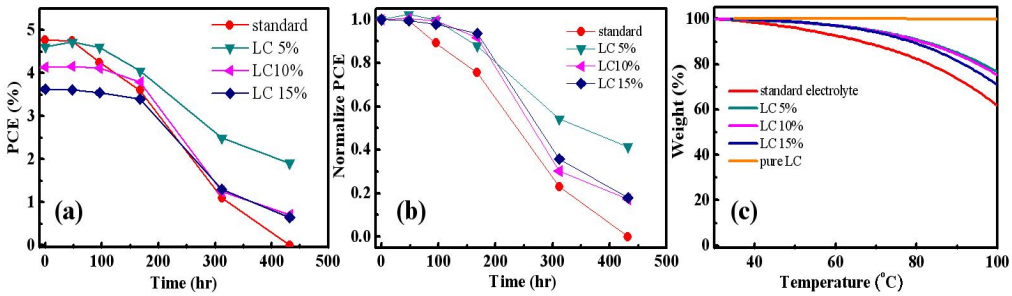

Fig. 4. (a) Long-term PCEs of the LC-doped DSSCs at various LC concentrations, (b) Normalize PCEs of the LC-doped DSSCs at various LC concentrations, (c) TGA curves of the LC-doped electrolytes at various LC concentrations and pure LCs.

The interaction between LCs and 3-MPN in the liquid electrolyte is a complex condition. Thus, a simple picture can be used to briefly explain the results. When the doped LC concentration is low, the LC molecules are fully dispersed and effectively interact with 3-MPN molecules because of the same cyano groups present, as shown in Figs. 1(b) and 1(c). Afterward, the LCs' rigid aromatic rings with cyano groups-attached increase the viscosity and thermal stability of the LC-doped electrolyte. When the doped LC concentration is high, the LC molecules are not completely dissolved by the 3-MPN molecules. Notably, LCs with similar molecules are inclined to bind with each other. The difference of the dielectric constants of E7 and 3-MPN is large; hence the difference of polarity between them is also large. Owing to this significant difference in polarity, the doped LCs are inclined to bind with one another, thereby preventing 3-MPN from effectively interacting with LCs. Consequently, the stability of the liquid electrolyte degrades when the doped LC concentration is high.

Notably, even in a well-sealed cell after a long-term operation, previous studies still reveal that liquid electrolytes are easily volatilized and leaked out, which reduces the light-to-electrical energy conversion efficiency of DSSCs [17, 37, 38]. Additionally, the rapid evaporation of the liquid electrolytes often causes practical limitations during the sealing process of the liquid solar cells. Reducing the evaporation rate of the liquid electrolyte is

#255320 Received 14 Dec 2015; revised 28 Feb 2016; accepted 2 Mar 2016; published 4 Mar 2016

effective to improve the life time and yield rate of liquid solar cells. The obtained results indicate that a minute amount of LC molecules effectively interact with the organic solvent, thereby suppressing the evaporation rate of the liquid electrolyte. As reported [21–23], the efficiency of quasi-solid state DSSCs are improved by massive doping of LCs because the conductivity of electrolyte is changed by the order of LC materials. However, a minute of amount LC dopant do not change the order of the liquid electrolyte in this study. Consequently, the polarity and molecular structures of LCs are key factors that improves the stability of the liquid electrolyte. A minute amount of commercially available LC without cyano terminal group was also doped into the liquid electrolyte to fabricate DSSCs. However, the phase separation between 3-MPN and LC appeared, indicating the necessity of the polar cyano group of E7 molecules in this paper. The slow loss of the electrolyte may have resulted from the high boiling point of E7. However, without effectively binding LCs with liquid electrolyte, the characteristics of LCs, including high viscosity and thermal stability cannot retain the life time of liquid electrolyte-based DSSCs.

4. Conclusions

This study presents a method of improving the stability of DSSCs by doping the liquid electrolyte with a minute amount of LCs, which comprised aromatic rings with terminally attached cyano groups. The *J–V* and EIS measurements indicate that the doped LCs reduce the J_{SC} of the DSSCs because the doped LCs decrease the electrochemical reaction rate of I_3^- reduction. The doped LCs reduces the degradation rate of DSSCs by interacting with liquid electrolytes, which consequently slow down evaporation rate of the liquid electrolyte. LC materials with aromatic rings and cyano groups have been widely investigated, making them commercially available materials. This paper opens up a new application besides displays for LC materials. Different types of LCs such as nematics, ferroelectrics, blue phases, LC monomers, and ionic LCs may have different conformations, and consequently, different effects on liquid electrolyte-based DSSCs. Furthermore, other materials with polar and aromatic groups may also contribute to retain the life time of liquid electrolyte-based DSSCs. More detailed studies are required.

Acknowledgment

This work was supported by the Ministry of Science and Technology of Taiwan (Contract Nos. MOST 101-2112-M-018-002-MY3, 104-2811-M-018-001, 103-2622-E-018-007-CC3, 102-2112-M-029-005-MY3, and 104-2112-M-018-003-MY3). The authors would like to thank Prof. Rong Ho. Lee of the Department of Chemical Engineering, National Chung Hsing University for valuable discussions.

#255320 Received 14 Dec 2015; revised 28 Feb 2016; accepted 2 Mar 2016; published 4 Mar 2016